Engineering Research Express

PAPER

Design of a multibeam metasurface antenna for LEO satellite communications payload

To cite this article: A V Chesnitskiy *et al* 2022 *Eng. Res. Express* **4** 045025

IOP Publishing Eng. Res. Express 4 (2022) 045025 https://doi.org/10.1088/2631-8695/aca318

Engineering Research Express

RECEIVED
21 August 2022

REVISED
31 October 2022

ACCEPTED FOR PUBLICATION
15 November 2022

PUBLISHED
23 November 2022

PAPER

Design of a multibeam metasurface antenna for LEO satellite communications payload

A V Chesnitskiy[1], A N Kosmynin[2], K N Kosmynina[3] and K V Lemberg[4]

[1] Rzhanov Institute of Semiconductor Physics, Russian Academy of Sciences, Siberian Branch, Novosibirsk, Russia
[2] MatrixWave LLC, Moscow, Russia
[3] Skolkovo Institute of Science and Technology, Moscow, Russia
[4] Federal Research Center 'Krasnoyarsk Science Center of the Siberian Branch of the Russian Academy of Sciences', Krasnoyarsk, Russia

E-mail: achesnitskiy@gmail.com

Keywords: metasuface antennas, multibeam, anisotropic impedance, LEO satellite canstellations, software defined RAN, 6G networks

Abstract

In this paper, we propose a novel method for synthesizing a multibeam metasurface antenna (MSA) for use in a space application - a payload component of a small satellite as part of a low Earth orbit (LEO) satellite communication constellation. MSA is synthesized using the holographic technique with a divergent phase distribution. Using this method, a low-cost multi-beam Ku-band antenna with seven flattened beams is developed. The results of the numerical simulation and experimental study of the proposed seven-beam MSA were presented. The gain of each beam is about 25 dBi, the aperture efficiency of the MSA is ~40%. Each individual beam had a separate feed point and its own inclination angle (0°, $\pm3.5^\circ$, $\pm7^\circ$, $\pm10.5^\circ$). This paper shows that the presented MSA is not inferior in its characteristics to similar solutions, but is more compact and lighter, and also allows the formation of complex radiation patterns.

1. Introduction

The development of multibeam and tunable metasurface antennas is driven by the extensive growth and development of wireless communication system technologies, the advent of millimeter waves in 5G terrestrial networks, and research on 6G communication systems [1–4]. This is facilitated by the emergence and unprecedented growth of low-Earth orbit (LEO) satellite constellations and high-altitude platform stations (HAPS) [5, 6]. Currently, satellite communication systems are evolving from classical repeaters to more complex satellites with onboard processing. The constellation network infrastructure is moving towards software-defined LEO satellite networks [7]. This method of networking unleashes the potential of multipath systems by separating the network data from the control plane. A dedicated secure control channel protects against data flow interruption when a GSM gateway subscriber moves from beam to beam. This architecture can be implemented using the flattened multibeam antenna proposed in this study.

To create the required partial zones with a uniform power flux density, it is necessary to form several beams with flattened shapes, as shown in figure 1. The literature describes several common methods for forming multibeam antennas. Traditionally, Butler matrices or Luneberg lenses have been used to form several beams [8–10]. The main disadvantages of using these methods are the high insertion loss, large sidelobes, and great difficulty in forming beams with overlap. Antenna structures implemented by any of these methods are difficult to manufacture and have large geometric dimensions; with an increase in the number of beams, a significant increase in cost occurs [11, 12]. Rothman lens [13] is another method to form several beams. This method has the advantage of low-cost, wide band, simple fabrication, but at the same time it has limited gain—typically it can't be more than 15–20 dB. Rothman lenses and antenna arrays based on this technique is used for radio location application, but for the communication it's not enough effective.

Metasurface antennas are an innovative alternative to existing methods, and can also be effectively used for beamforming [13–17]. This method compensates for the shortcomings of the methods mentioned earlier in the article, which is why it is worthy of attention. A metasurface is a two-dimensional metamaterial structure

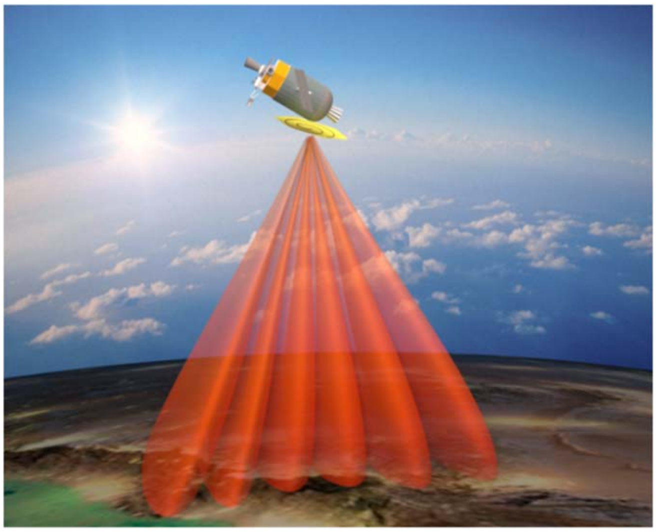

Figure 1. Concept of a multibeam antenna with flattened beams for low-orbit satellite constellation.

consisting of resonantly coupled subwave elements that exhibit unique electromagnetic properties. In recent years, tensor metasurfaces have been significantly developed for a wide range of applications in optoelectronics, semiconductor devices, communications, wireless power transfer, etc [18–20].

Metasurface antennas aren't currently common in space applications [21]. But the dramatically fast development of LEO constellations drives the development of lightweight and effective antenna systems which are able to form beams of different shapes and multibeam systems. The contribution of this study is the proposing of a potentially effective solution for uplink and downlink for LEO satellites. In current publications the possibility of forming a customized beam and beam steering systems was discussed [22].

The concept of forming metasurfaces with a tensor impedance distribution justified its validity and led to the design of a wide class of antenna structures in the millimeter and centimeter ranges [23]. In such structures, a surface cylindrical TM wave interacts with a periodically modulated surface of spatially varying artificial impedance from the subwavelength resonant elements. The physical mechanism of radiation from an open waveguide structure into free space is as follows: When a slow surface wave ($v < c$) interacts with a periodically changing impedance of the structure, it is transformed into a leaky wave (LW) mode ($v > c$). Radiation occurs at angle θ:

$$\sin\theta = \frac{c}{v_{\Phi}}, \tag{1}$$

where c is the speed of light and v_{Φ} is the phase velocity of the $n = -1$ Floquet harmonic (FH) of the surface wave.

The key feature of a tensorial metasurface is the opportunity to obtain the desirable polarization, amplitude, and shape of the wavefront radiation [24, 25].

The main advantages of MSA are its simple manufacturing, low profile, and light weight compared with other types of antennas. With one or more feed points, it is possible to excite one to several beams with smaller geometric antenna dimensions. The aperture of a planar MSA is typically tens of wavelengths, and its thickness is a few millimeters. In this paper, we propose implementations of the multisource feeding scheme of multibeam MSA with an original flattened beam shape for use in satellite communication payloads [26]. The use of anisotropic surface impedances enables the maintenance of a large aperture and the manipulation of the radiation phase at the aperture. The synthesis technique proposed in this study differs from these methods.

2. Beam forming

In our opinion, the most optimal approach to design a multibeam MSA for satellite payloads is to superimpose several distributions, each of which forms a separate beam, with all beams added to an array covering a large area of the Earth's surface. The arrangement of distributions fits into a hexagonal grid for the most efficient filling of the antenna area. It is known that the hexagonal grid has the highest fill factor, which will allow to achieve the smallest sizes, as well as owing to mixing MSA patterns.

The direction, intensity, and polarization of the radiation of slow surface waves can be controlled by setting the required modulation of the tensor impedance. The surface impedance tensor $\hat{Z}_s$ describes the

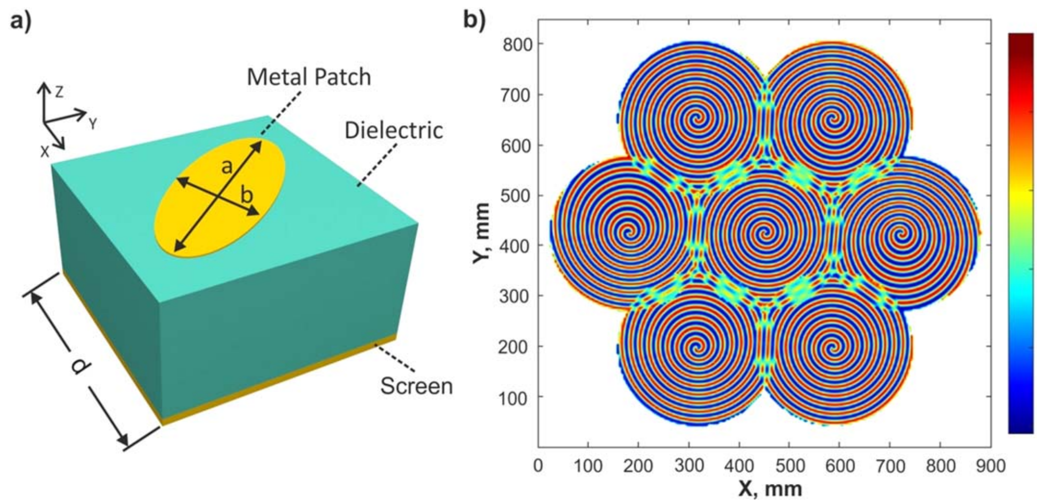

Figure 2. Synthesis of multibeam antennas with flattened beams: (a) Geometry of anisotropic unit cell with dimensions $0.12\lambda_0 \times 0.12\lambda_0$; (b) Impedance distribution of the $Z_{\rho\rho}$- surface tensor component of seven-beam MSA.

electromagnetic properties of the metasurface, as follows:

$$\hat{Z}_s = \begin{bmatrix} Z_{uu} & Z_{uv} \\ Z_{vu} & Z_{vv} \end{bmatrix}, \tag{2}$$

where u and v are the unit vectors of the coordinate system selected on the surface. The relationship between the tangential component of electric E_t and magnetic H_t fields is given by the following expression:

$$E_t = Z_s \times [n \times H_t], \tag{3}$$

where n is a unit vector directed along the normal to the surface.

Thus, the tensorial character of impedance makes it possible to relate the orthogonal components of the fields on the surface. Sinusoidal modulation of the impedance leads to the appearance of additional FH radiating into open space. Previously, we developed an algorithm for the synthesis of metasurfaces, which was described in detail in [27, 28]. The procedure for synthesizing a metasurface consisting of subwavelength, elements includes the following steps: (1) calculation of the tensor cell impedance values, (2) calculation of the required distribution of the tensor impedance components on the surface, and (3) building the antenna canvas.

In this study, a synthesis method based on a holographic approach is used. It was previously shown that MSA with anisotropic tensor impedance has a significantly higher aperture efficiency than isotropic ones, owing to the low level of cross-polarized fields [29, 31]. Therefore, to set the anisotropy of the structure, various sizes, shapes, and directions of metal patches were used. In this work, we have chosen patches in the form of ellipses (figure 2(a)). The patches are arranged in square unit cells, with the cells having a size d of less than a quarter of a wavelength in the waveguide structure in order for the surface to be effectively continuous. In practice, the dimension d may be from 1/10 to 1/5 of the wavelength in the waveguide structure. In the work, the dimensions of the unit cell of the synthesized MSA were chosen as 1/8 of the wavelength ($0.12\lambda_0 \times 0.12\lambda_0$). The components of the impedance tensor were modulated by their average values according to the following equation:

$$Z_{ab} = \bar{Z}_{ab} + \frac{\Delta Z_{ab}}{2} \cdot Re\left(\frac{E_{(obj)a} E^{*}_{(ref)b}}{|E_{ref}|^2}\right), \tag{4}$$

where indices a and b are the coordinates of the point in cylindrical coordinates ρ, φ, E_{obj}, E_{ref} are the electric field strength of the object and reference waves, respectively; $\bar{Z}_{ab} = \bar{Z}_{\rho\rho}$, $\bar{Z}_{\varphi\varphi}$, $\bar{Z}_{\rho\varphi}$, $\bar{Z}_{\varphi\rho}$ are the average values of the impedance component implemented by cells; $\Delta Z_{ab} = \Delta Z_{\rho\rho}$, $\Delta Z_{\varphi\varphi}$, $\Delta Z_{\rho\varphi}$, $\Delta Z_{\varphi\rho}$ are the ranges of values of the corresponding impedance component. Because the impedance tensor described earlier is diagonal for mutual media, only two components $Z_{\rho\rho}$ and $Z_{\rho\varphi}$ determine the surface properties.

Using this synthesis algorithm with numerical simulations, a wide range of radiation patterns can be obtained. Specially designed radiation patterns are often required for satellite communication and distributed Earth coverage. For instance, the formation of a multibeam MSA with deflected flattened beams is topical. In the general case, with a uniform phase distribution on the emitting aperture, the beam width depends on the aperture size, which is expressed in wavelength λ_0. It is known that if the aperture in two dimensions is different, the beam will broaden in smaller dimensions. Slotted waveguide antennas with different aperture sizes in two directions have already been used in practice for beam shape design in a number of practical applications [32].

We propose a novel method for forming flattened beams based on the phase variation on the surface of the MSA aperture. The metasurface synthesis method is based on setting the phase front of a wave to diverge in one plane. The object wave is given as:

$$E_{(obj)} = A_{(obj)} e^{-jk_0\rho \sin\varphi \cdot \sin\theta_0} \times e^{-jk_0 r\left(\sqrt{\left(\frac{1}{\xi}\right)^2 - \left(\frac{\rho}{r}\right)^2 \varphi} - \sqrt{\left(\frac{1}{\xi}\right)^2 - \varphi}\right)}, \quad (5)$$

where ρ is the radius vector of a point on the surface, r is the radius of the antenna, and ξ is a coefficient that specifies the convexity of the phase front.

The first exponential term in equation (5) describes a flat phase front with a slope in the YZ plane corresponding to angle θ_0. The second exponential term describes the additive in the form of a phase-front convex curve in the XZ plane. By varying the parameter ξ, an extended beam was formed in this plane. At $\xi = 0$, the phase front was not convex (flat), and the beam did not expand. When $\xi = 1$, it has a bulge with a radius equal to the electrical radius of the antenna, and the beam has maximum expansion in the XZ plane. In this case, the front in the other direction remained flat, and the aperture sizes were the same in both directions. The united canvas is formed by mixing grains at the boundaries of the individual patterns. Multipath excitation with sparse feed points can be observed by combining multiple impedance distributions on a large canvas. In this case, each radiated wave will have a radiation angle deviation and a beam width. It is possible to receive several beams simultaneously from one canvas with single feed point, but this leads to a corresponding decrease in the gain [30]. The obtained surface distribution of the component of the impedance tensor for a seven-beam MSA with separate feed points is shown in figure 2(b). Negligible impedance perturbations are visible at the pattern boundaries when mixing individual distributions during synthesis. The degree of the multiplexing method can be set during the synthesis of the multibeam antenna. The proposed method makes it possible to significantly reduce the final size of the aperture without reducing the efficiency owing to pattern mixing. In the experiment, to demonstrate the approach, we fabricate only a part of the canvas with the largest inclination angle.

3. Numerical results

An illustration of the synthesized seven-beam MSA with right circular polarization is shown in figure 3. Numerical simulation of radiation patterns in the far zone and electrical parameters of the synthesized multibeam MSA were performed using the finite element method (FEM). The model includes the parameters of the widely used inexpensive dielectric FR4 ($\varepsilon_r = 4.5$, $tg\delta_\varepsilon = 0.022$). FR4 might be exchanged with another dielectric substrate material with the closest value of dielectric permittivity and lower loss tangent. In this research FR4 was used mainly due to its chip price, but in commercial applications more advanced material might be used (Relong RC450, Wangling F4BTM-1/2, Taconic RF-45, Arlon AD450). The proposed planar antennas can be implemented using traditional printed circuit board (PCB) technology, which is compatible with the mass production of two-layer copper-plated PCBs. The aperture dimensions of the fully flattened beam antenna were $34\lambda \times 31\lambda$ at a central frequency of 12 GHz, and the thickness of the dielectric substrate is 2 mm.

Inclination angles have been selected and optimized to maximize coverage and achieve signal uniformity. In ideal case, it is planned to create a zone of equal flux power on Earth surface by overlapping the beams at the same level. The level of overlap in the experiment will depend on the angles of inclination and the width of each of the beams. The graph (figure 4) shows the directions of the main lobes of the designed seven-beam MSA. The calculated gain (G) for the radiation angle of 0°, ±3.5°, ±7°, ±10.5° was 24.3 dBi, 24.8 dBi, 24.7 dBi and 24.5 dBi, respectively. A small spread between the gain values on the canvas for different beams ($\Delta G < 3\%$) indicates high reproducibility of the results of the synthesis of the impedance distribution over the surface. It can be seen from the graph that all beams overlap at a level of more than −3 dBi.

4. Experimental results

For experimental verification of the proposed method, samples of one element of a multibeam MSA were fabricated using the PCB method from the FR4 dielectric. Figure 5(a) shows a photograph of the realized single-beam MSA with a flattened beam shape. The figure shows the feeding waveguide and assembled antenna. A feeder in the form of a pin with a disk was used to excite a TM-type surface wave, and an SMA connector was used to connect it. The overall dimensions were 380 mm × 380 mm.

We performed measurements of the radiation pattern of single-beam antenna with an oblique beam in an anechoic chamber. The color map shown in figure 5(b) is a three-dimensional (3D) image of the radiation pattern of the fabricated single canvas. The antenna radiated with a circular polarization of 24.5 dBi at a frequency of 12 GHz. Thus, the aperture efficiency of the proposed planar structure was 40%. It can be seen from

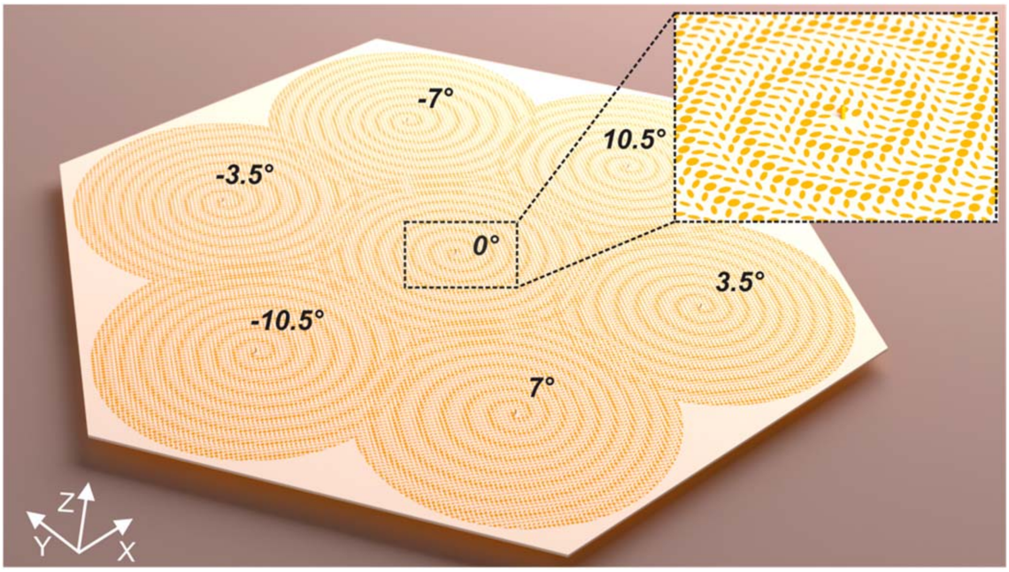

Figure 3. Schematic view of designed seven-beam MSA. The inset shows the metal patches in detail.

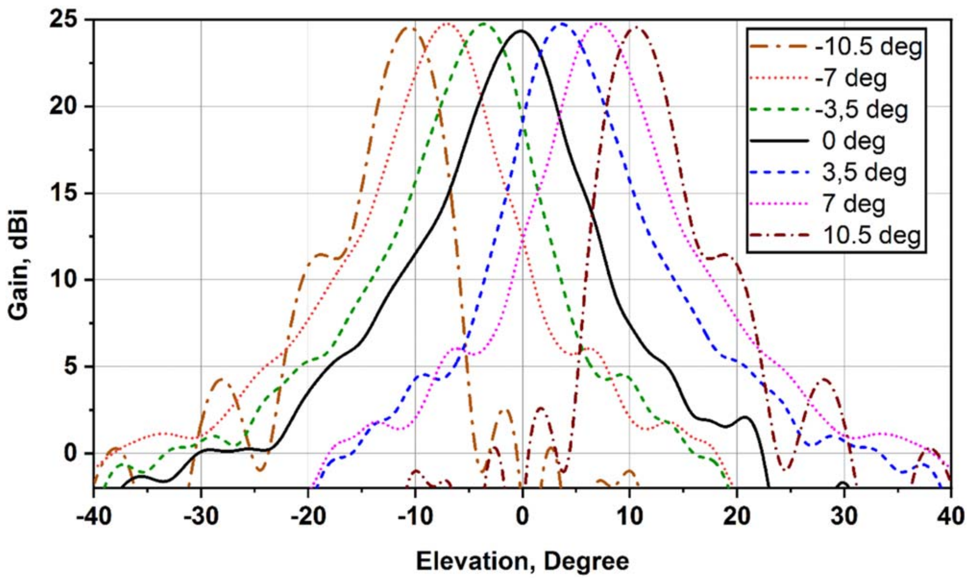

Figure 4. Simulated far-field radiation patterns of seven-beam MSA at 12 GHz.

the figure that the beam has an elongated shape in the XZ plane, good symmetry, and is tilted in the required direction by an angle of 10.5°.

Scattering parameter |S11| with respect to frequency is shown in figure 6. Return loss is less than −18 dB at the center frequency and is suitable for typical space applications.

Figures 7(a) and (b) demonstrate a detailed sectional plane of the far-field radiation pattern in azimuth and elevation, respectively. It can be seen that the radiation pattern has the shape of a beam elongated in the elevation direction. Such a result was obtained due to the divergent phase distribution of the surface impedance created at the synthesis stage in this direction. The results obtained from the finite element simulation for the fabricated MSA are superimposed on the graphs and shown with dotted lines for comparison. There is a close agreement between the measured and simulated results in the main beam region, and there is also a slight discrepancy due to the limitation of the computer's computing capabilities and the use of a simplified structure mesh in the calculation process. From the graphs below, the angular widths ($\Delta\theta$) of the main lobe at the level −3 dB were obtained, and they were 4.5° and 16° in two directions, respectively.

The graphs in figures 7(c) and (d) show the dependences of the cross-polar component of the radiation pattern in the azimuth and elevation, respectively.

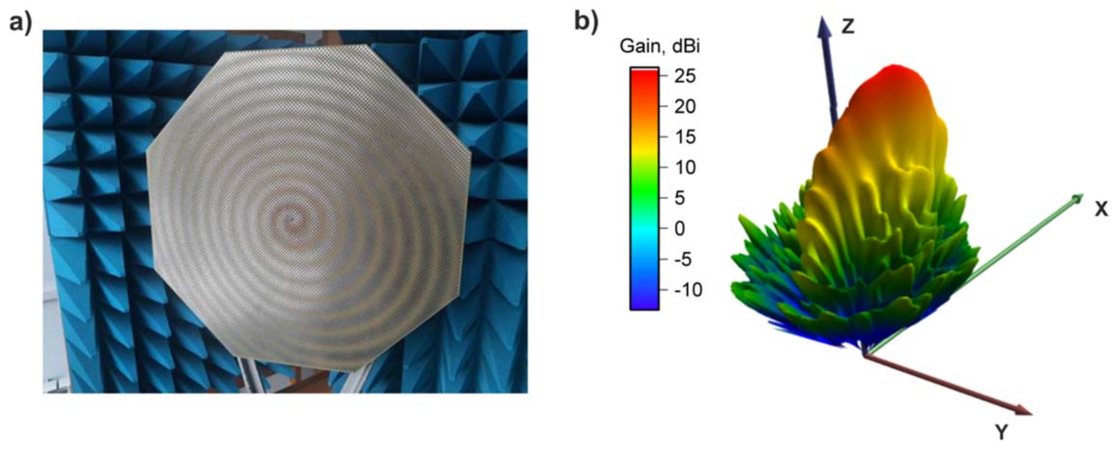

Figure 5. MSA with a single flattened beam at an angle of 10.5° (a) Photograph of the fabricated prototype; (b) Measured 3D far-field radiation pattern at 12 GHz.

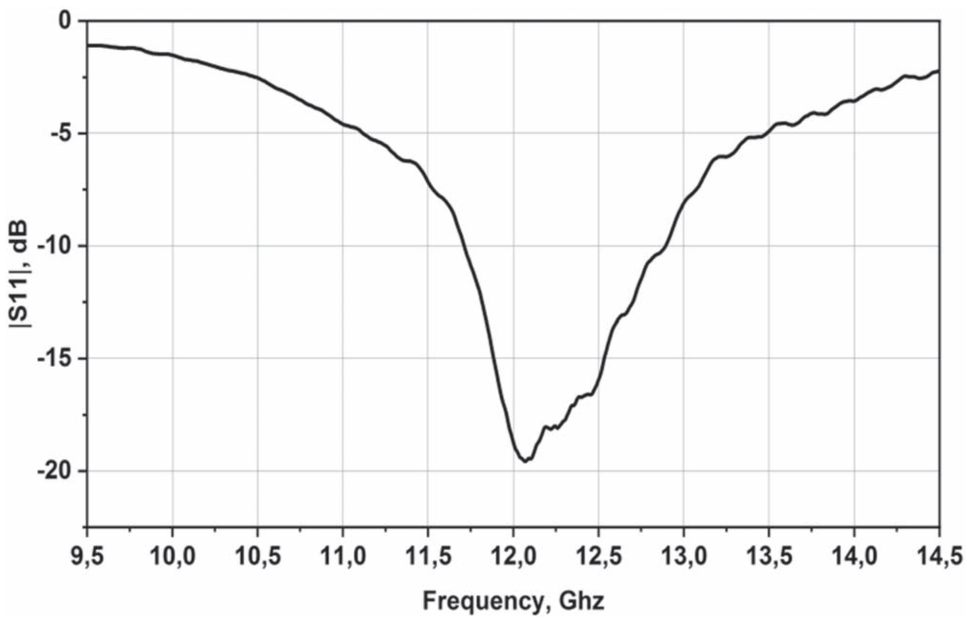

Figure 6. Measurement of the return loss with respect to the frequency

It can be seen from the graphs that the measured cross-polar discrimination is about −13 dB in both directions. The cross-polarization value can be further reduced, and the gain can be increased by optimizing the structural parameters and carefully shaping the sub-resonant metal patches [31]. In addition, in the manufacturing of the proposed MSA for LEO applications, it is necessary to use PCB on commercially available microwave dielectrics with a small loss tangent that do not emit halogens under harsh conditions. Such dielectrics are widely used in an avia satellite production due to its high resistance to any kind of disturbances (power, temperature, humidity, pressure). The antenna itself is made of the dielectric substrate and metallic patches, so it's sustainable and applicable for space industry.

Furthermore, using the obtained values of angular widths, it is possible to calculate the geometric parameters of the coverage area of the Earth's surface, according to the following formula:

$$L = tg(\Delta\theta) \cdot h, \tag{6}$$

where h is the orbit height.

With the satellite orbit height h = 500 km, the calculated length and width of the spot on Earth are ≈143 × 39 km.

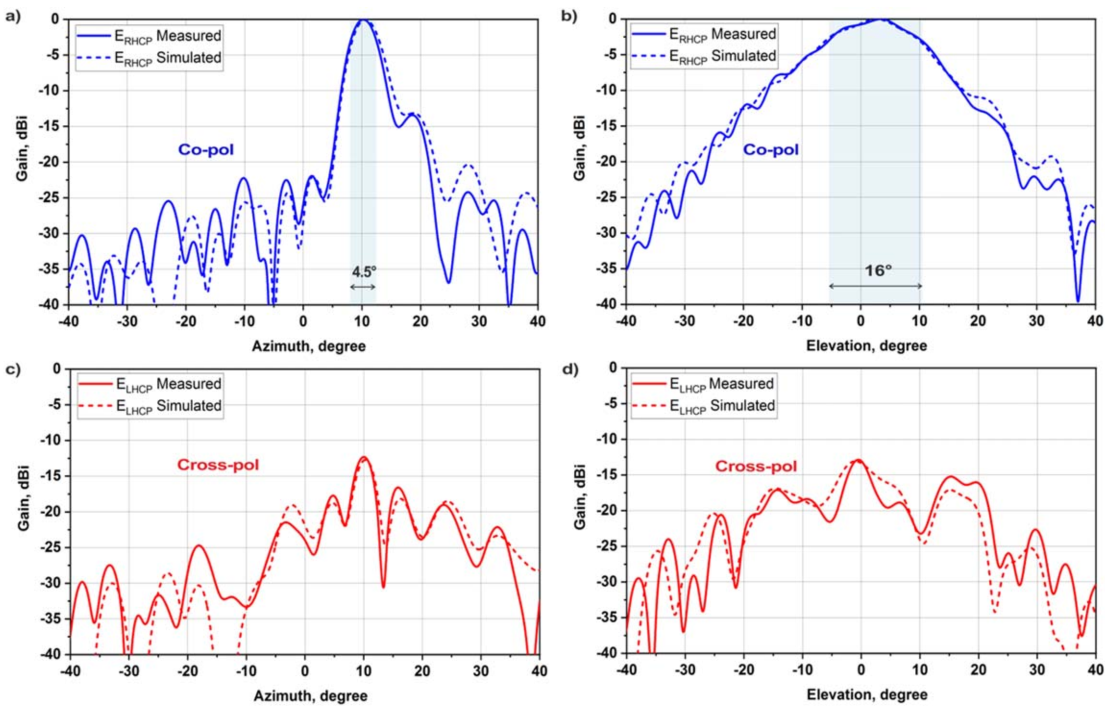

Figure 7. Sections of measured (solid lines) and simulated (dashed lines) radiation patterns (normalized) at 12 GHz: (a) RHCP component at elevation = 0°; (b) RHCP component at azimuth angle = 10.5°; (c) LHCP component at elevation = 0°; (d) LHCP component at azimuth angle = 10.5°. The shaded area in graphs (a) and (b) schematically shows the beamwidth in two directions at −3 dB.

In the article [32] the budgeting of the power of LEO satellites was investigated and described. The authors are looking at the low Earth orbit power budget to see if the MSA produced could be suitable for the high power in the LEO application constellation. The use of antennas based on metasurfaces manufactured using PCB technology will make it possible to supply power without damage from 11 W to 30 W to solve these problems.

Designed multibeam MSA in the future may find application in the rapidly developing field of next-generation 5/6G networks [33], low-orbit communication spacecraft, pseudo-satellite platforms HAPS, and unmanned aerial vehicles (UAVs) [34, 35]. Considering the requirements to minimize the mass of spacecraft, the presented approach to multibeam antenna design is one of the most promising and interesting.

5. Conclusion and prospects for the future

This paper demonstrates an improved design of a multibeam MSA with the possibility of forming a flattened radiation pattern. Using numerical simulation methods, the radiation patterns of tensorial multibeam MSA with inclination angles (0°, ±3.5°, ±7°, ±10.5°) were obtained, and their characteristics were studied. A prototype of the Ku-band range of a canvas element with an expanded beam in one direction and a tilt angle of 10.5° was fabricated. An experimental study of its characteristics and radiation patterns was conducted, and it was shown that the gain reached 24.5 dBi and aperture efficiency of the sheet was 40%. The experimental results are in good agreement with the results of the numerical simulation. The proposed technique is shown to be promising for designing next-generation 5/6G networks and LEO communication systems.

Acknowledgments

The experimental research was carried out with the financial support of the RFBR, the Government of the Krasnoyarsk Territory and the Krasnoyarsk Regional Science Foundation within the framework of the scientific project 20–47–243002.

Data availability statement

All data that support the findings of this study are included within the article (and any supplementary files).

Competing interests

All authors declare that they have no competing financial interests.

ORCID iDs

A V Chesnitskiy https://orcid.org/0000-0002-6860-8974

References

[1] Bodehou M, Martini E, Maci S, Huinen I and Craeye C 2019 Multibeam and beam scanning with modulated metasurfaces *IEEE Trans. Antennas Propag.* **68** 1273–81

[2] Bao L, Wu R Y, Fu X, Ma Q, Bai G D, Mu J, Jiang R and Cui T J 2019 Multi-beam forming and controls by metasurface with phase and amplitude modulations *IEEE Trans. Antennas Propag.* **67** 6680–5

[3] Dai H, Zhao Y and Yu C 2020 A multi-elements chessboard random coded metasurface structure for ultra-wideband radar cross section reduction *IEEE Access* **8** 56462–8

[4] Nahar T and Rawat S 2022 Survey of various bandwidth enhancement techniques used for 5G antennas *Int. J. Microwave and Wireless Tech.* **14** 204–24

[5] Hong W *et al* 2017 Multibeam antenna technologies for 5G wireless communications *IEEE Trans. Antennas Propag.* **65** 6231–49

[6] Yurduseven O, Lee C, Gonzales-Ovejero D, Ettore M, Sauleau R, Chattopadhyay G, Fusco V and Chachat N 2020 Multi-Beam Si/GaAs holographic metasurface antennas in the W-band *IEEE Trans. Antennas Propag.* **69** 3523–8

[7] Xu S, Wang X W and Huang M 2018 Software-defined next-generation satellite networks: architecture, challenges, and solutions *IEEE Access* **6** 4027–41

[8] Chen J, Chu H, Huang Y, Lai Y and Chen M 2022 Ultra-wideband luneburg lens with high performance based on gradient metamaterials *J. Phys. D: Appl. Phys.* **55** 355109

[9] Butler J 1961 Beam-forming matrix simplifies design of electronically scanned antennas *Electron. Des.* **9** 170–3

[10] Xiao Y and Ye S 1995 Wide-band lens multi-beam antenna *Warship Electronic Countermeasures* **6** 23–9

[11] Tajik A, Alavijeh A S and Fakharzadeh M 2019 Asymmetrical 4 × 4 Butler matrix and its application for single layer 8 × 8 Butler matrix *IEEE Trans. Antennas Propag.* **67** 5372–9

[12] Kuang Z, Zhang K, Liu Z and Li Z 2018 Design method of lens multi-beam antenna based on Quasi-optics *Electronic Information Warfare Technology* **6** 71–5

[13] Zongxin W, Bo X, Fei Y and Multibeam A 2013 Antenna array based on printed rotman lens *International Journal of Antennas and Propagation* **2013** 1–6

[14] Teniou M, Roussel H, Serhir M, Capet N, Piau G P and Casaletti M 2018 Tensorial metasurface antennas radiating polarized beams based on aperture field implementation *Int. J. of Microwave and Wireless Tech* **10** 161–8

[15] Gonsalez-Ovejero D, Minatti G, Chattopadhyay G and Maci S 2017 Multibeam by metasurface antennas *IEEE Trans. Antennas Propag.* **65** 2923–30

[16] Minatti G, Caminita F, Martini E, Sabbadini M and Maci S 2016 Synthesis of modulated-metasurface antennas with amplitude, phase, and polarization control *IEEE Trans. Antennas Propag.* **64** 3907–19

[17] Chesnitsky A V, Kaigorodov O M, Kosmynina K N, Kosmynin A N, Sibirtsev P A and Lemberg K V 2022 Multibeam antenna implementation using anisotropic metasurfaces *IEEE 23rd International Conference of Young Professionals in Electron Devices and Materials (EDM)* 2022 (IEEE) 251–5

[18] Glybovski S B, Tretyakov S A, Belov P A, Kivshar Y S and Simovski C R 2016 Metasurfaces: from microwaves to visible *Phys. Rep.* **634** 1–72

[19] Hu J, Bandyopadhaya S, Liu Y and Shao L 2021 A review on metasurface: from principle to smart metadevices *Front. Phys.* **8** 502

[20] Chen S, Zhou X, Guo Q and Ye H 2019 Two-dimensional material and metasurface based optoelectronics *Adv. Condens. Matter Phys.* **2019** 1–2

[21] Minatti G, Caminita F, Martini E, Martorelli V, Benini A, Le Coq L and Maci S 2018 Ka-band metasurface antenna for data downlink from LEO satellites *12th European Conf. on Antennas and Propagation (EuCAP 2018)* 1–3

[22] Zhang H *et al* 2022 Multibeam antennas with customized elevation angles based on near-field magnetic field coupling of metamaterials *J. Phys. D: Appl. Phys.* **55** 43LT01

[23] Smith D R, Yurduseven O, Mancera L P and Bowen P 2017 Analysis of a waveguide-fed metasurface antenna *Phys. Rev. Appl.* **8** 054048

[24] Faenzi M, Graziuso N, Martini E and Maci S 2022 Design methods for dual polarized metasurface antennas: three simple approaches *IEEE Antennas Propag. Mag.* **64** 37–50

[25] Dong J, Wu R and Pan Y 2022 A low-profile broadband metasurface antenna with polarization conversion based on characteristic mode analysis *Front. Phys.* **10** 122

[26] Braun T M 2012 *Satellite Communications Payload and System* (Hoboken, NJ: Wiley) 720

[27] Lemberg K V, Kosmynin A N, Aleksandrin A M, Grushevsky E O and Podshivalov I V 2021 Method of anisotropic metasurface unit cell surface impedance calculation *IEEE Radiation and Scattering of Electromagnetic Waves (Divnomorskoe, Russia)* 273–275

[28] Lemberg K V, Grushevsky E O, Podshivalov I V, Kosmynin A N and Kosmynina K N 2021 Synthesis method and experimental research of ku-band antennas based on tensorial metasurfaces *Journal of Siberian Federal University, Engineering & Technologies* **14** 840–53

[29] Minatti G, Faenzi M, Martini E, Caminita F, De Vita P, González-Ovejero D, Sabbadini M and Maci S L 2015 Modulated metasurface antennas for space: synthesis, analysis and realizations *IEEE Trans. Antennas Propag.* **63** 1288–300

[30] Barnett J R 2018 *Oneweb Non-Geostationary Satellite System: Attachment a—Technical Information to Supplement Schedule S* (Washington, DC: Federal Commun. Commission)

[31] Faenzi M, Minatti G, González-Ovejero D, Caminita F, Martini E, Della Giovampaola C and Maci S 2019 Metasurface antennas: New models, applications and realizations *Sci. Rep.* **9** 1–14

[32] Ali A J *et al* 2021 Power budgeting of LEO satellites: an electrical power system design for 5G missions *IEEE Access* **9** 113258–69
[33] Wang Z and Dong Y 2022 Metamaterial-based, vertically polarized, miniaturized beam-steering antenna for reconfigurable sub-6 GHz applications *IEEE Antennas Wirel. Propag. Lett.* **21** 2239–43
[34] Harrop P, Dyson M, Edmondson J and Das R 2021 6G Communications Reconfigurable Intelligent Surfaces Roadmap, Materials, Market 2021-2045 *Research Report* 328
[35] Kurt G K, Khoshkholgh M G, Alfattani S, Ibrahim A, Darwish T S J, Alam M S, Yanikomeroglu H and Yongacoglu A 2021 A vision and framework for the high altitude platform station (HAPS) networks of the future *IEEE Communications Surveys & Tutorials* **23** 729–79